Dendritic growth of ammonium chloride crystals: Measurements of the concentration field and a proposed nucleation model for growth

Eli Raz, S. G. Lipson, and E. Polturak
Department of Physics, Technion–Israel Institute of Technology, Haifa 32000, Israel
(Received 19 January 1989)

We have developed a method of investigating the solute concentration field around a dendrite growing from a supersaturated ammonium chloride solution. It uses the refractive index of the solution as a measure of its concentration. The spatial dependence of refractive index is measured with the aid of an interference microscope. The field distributions obtained in this way indicate a nonlinear relationship between growth velocity and driving force. We propose a model for dendritic growth based on homogeneous nucleation at a temperature below the surface roughening temperature. We show that it is consistent with the measurements and also provides a mechanism of pattern selection.

INTRODUCTION

Dendritically growing crystals, which present a dramatic example of spontaneous pattern formation, have been the subject of many investigations during the past decade. Although there is a broad understanding of the ingredients needed for a complete modeling of the situation,[1,2] there still seem to be many open questions regarding the way in which the material parameters control the shape of the dendrite eventually observed. It is clear from the experimental work and simulations carried out in many laboratories that diffusion, either of solute or latent heat and in many cases both, is one of the controlling themes. In addition, surface tension and growth dynamics, both of which are generally anisotropic, play important parts. It is the role of the last of these which is our main topic.

The experiments described in this paper were designed to measure the solute diffusion field around a growing dendrite of NH_4Cl, and we have found that they support a model for dendritic growth of this material which is based on the dynamics of crystal growth by nucleation on atomically smooth facets, and which results in a natural explanation of the pattern formation. A requirement of this approach is that a crystal surface in the direction of growth is below its surface roughening temperature T_R, which we believe to be true for the crystals in our experiments. Mauer *et al.*[3] estimate the roughening temperature of NH_4Br to be in the region of 70–90 °C. However, the generality of the model remains an open question, since little is known about the surface roughening temperatures of crystals in general. The experiments support the model through direct measurements of the nonlinearity in the growth kinetics and by the observation of periodic variations in the tip velocity.

EXPERIMENTAL METHOD

Almost all of the work done to date has concentrated on an investigation of the morphology of the growth shapes (for example, spacing between side branches, radius of curvature) and their evolution with time (e.g., tip velocity). Two systems which have been widely used in experimental work are succinonitrile, growing from the melt,[4] and ammonium halides, crystalizing from solution.[3,5–8] The system we selected for our investigation was ammonium chloride growing from a supersaturated solution, for which basic data exist[9] as well as other experiments on dendritic growth. The crystals were grown in a cell between a glass plate and a mirror separated by a variable distance and in contact with a heat bath. The solute concentration field in the liquid around the growing crystal was measured from the shift of the fringes which cross the field when the cell is observed in an interference microscope. This technique measures the integrated quantity of solute in the cell along a line normal to the cell faces, in a manner which does not disturb the crystal growth in any way.

The results, whose estimated accuracy was about 0.3% of the concentration, were then compared with the predictions of a model describing the solute field around the dendrite, based on an assumption of isotropic growth and uniform saturation concentration of solute on the surface of the dendrite. Although the cell is quasi-two-dimensional, the growth of the dendrite tip was assumed to be three dimensional, since its typical dimensions were considerably smaller than the thickness of the cell. Several morphological phenomena associated with the restricted vertical dimension of the cell were discovered while carrying out experiments in the thinnest cells, but since these were not relevant to the present study they will be reported separately.[10]

Figure 1 shows a schematic diagram of the experimental system. The cell has an outside diameter of 28 mm. Its base is built primarily of copper and is maintained by flowing water at a constant temperature, to an accuracy of about 0.2 °C. A thin mirror (0.17 mm thick), aluminized on its lower surface, is cemented onto it. The temperature of the copper plate is measured with a copper-constantan thermocouple. We determined that, after a small correction (about 0.3 °C) has been made for a temperature gradient across the mirror, this thermocouple

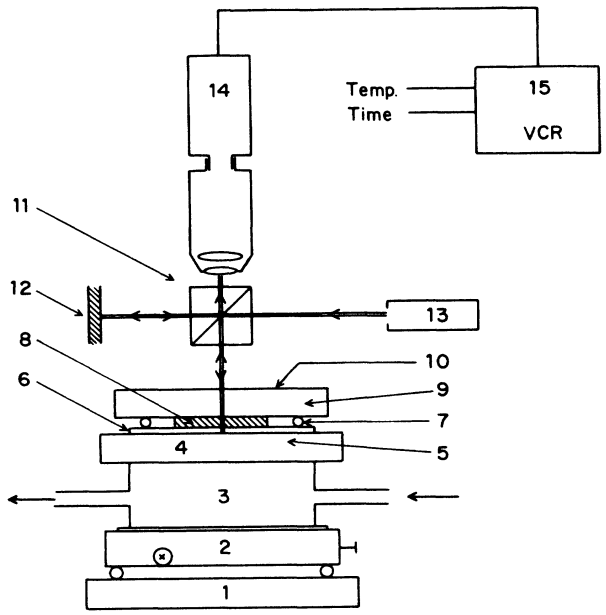

FIG. 1. Experimental system: 1, microscope stage; 2, tilting table; 3, water-cooled chamber; 4, copper cell base; 5, thermocouple; 6, thin mirror; 7, spacers; 8, sample solution; 9, microscope slide; 10, flowing nitrogen; 11, interference microscope; 12, adjustable reference mirror; 13, sodium lamp; 14, television camera; 15, VCR.

gives the temperature of the solution (the subject of temperature variations within the cell due to the growth process will be discussed later). The thickness of the sample is determined by two identical spacers which are placed on the mirror, and is known to an accuracy of 1–2 μm. Spacers between 20 and 160 μm were used. The upper window of the cell is a microscope slide 1 mm thick, above which dry nitrogen gas flows slowly so as to prevent condensation of water from the air when its temperature is below ambient.

The cell is observed through an interference microscope, which is essentially a Michelson interferometer in which the cell-base mirror replaces one of the interferometer mirrors. The illumination is by a sodium lamp, which is preferable to a laser because its shorter coherence length prevents formation of spurious fringes. The microscope image shows interference fringes which represent contours of constant phase difference between the two arms of the interferometer; it is observed either visually or with a video camera and a television monitor and is recorded on video tape. The latter also records simultaneously time and cell temperature. Because of the limited depth of field of the microscope, the cell is mounted on a tilting table which is adjusted so that it remains in focus throughout mechanical scanning of the complete region of interest.

We prepared solutions of high-purity (99.999%) ammonium chloride in distilled water with concentrations of between 27 and 31 wt. %. The saturation temperatures of these solutions are 19.5 and 38.9 °C, respectively (Fig. 2). For each experiment we placed a drop of the thoroughly mixed solution on the mirror base and closed the cell while it was maintained above the saturation temperature. We then used the water cooling to reduce the temperature, obtaining initial supercoolings of between 10 and 25 °C, and initiated crystallization by a slight tap.

We can calculate the concentration field from the interference pattern as follows. First of all, before crystallization begins the tilt of the interferometer reference mirror has been adjusted to give a convenient arbitrary set of straight-line fringes represented by phase

$$\phi_0(\mathbf{r})=\alpha\mathbf{r} \ , \tag{1}$$

where α is a known constant and $\mathbf{r}$ is the position vector in the plane of observation. In a given interferogram, the phase is

$$\phi(r)=\phi_0+2\int_0^Z[n(x,y,z)-n_0]k_0dz \ , \tag{2}$$

where $k_0=2\pi/\lambda$ is the free-space wave number of the light and $n(x,y,z)$ is the local refractive index. The refractive index in the initial state (straight-line fringes) is n_0. The factor 2 preceding the integral arises because the light traverses the cell twice. Z is the cell thickness. Since the fringes are contours of constant phase, the variations in phase $\delta\phi=\phi(r)-\phi_0$ from (2) appear as distortions of the original straight fringes where one complete fringe shift corresponds to 2π phase change.

If there were no changes in n in the z direction (uniform concentration throughout the thickness of the cell) we should have from (2) a direct relationship between the refractive index and phase change:

$$\delta\phi=2Zk_0[n(x,y)-n_0] \ . \tag{3}$$

At a given temperature the refractive index of the solution is linearly related to the concentration C of the solute:

$$n=n_0+mC \ . \tag{4}$$

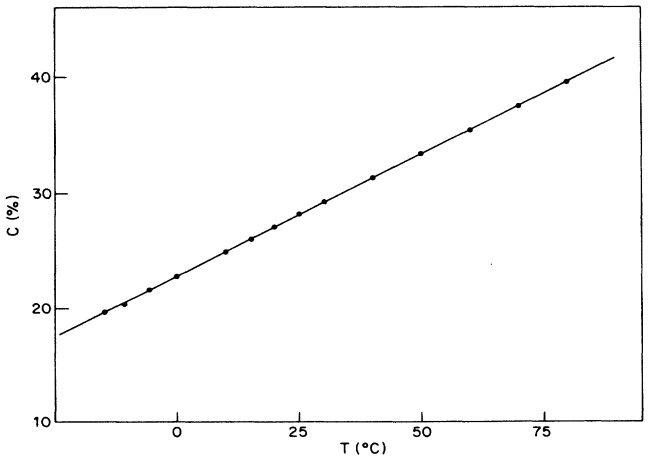

FIG. 2. Phase diagram of NH_4Cl in the (C,T) plane (after Ref. 9).

We determined m with the aid of an Abbe interferometer; the values, which were insignificantly different from those in the literature,[9] were, for $\lambda=5893$ Å, $n_0=1.3325-0.00013(T-25\,^\circ\text{C})$ and $m=0.190$ per unit weight fraction. The concentration change δC is related to $\delta\phi$ by

$$\delta C=\delta\phi\lambda/4\pi Zm \ . \tag{5}$$

If we assume that a sensitivity of 0.1 fringe can be achieved in measuring displacements, a minimum change of $\delta C=(\lambda/20)Zm$ can be detected. Computer imaging-processing techniques could possibly improve the sensitivity of the technique by a further two orders of magnitude, but have not been employed in the present work.

Since the refractive index is sensitive to both temperature and concentration, it is necessary to assess the relative influence of these two fields on the measurements. We can show that under typical experimental conditions the temperature field can be neglected. First, in a dendrite freely growing from an infinite solution, the interface conditions may be at any point on the coexistence curve, the determination of which point can be carried out for a paraboloidal dendrite tip[11] and we find that, typically, the temperature difference between the interface and the bulk fluid is of order 0.15 °C; i.e., most of the supercooling is in the concentration field. Moreover, the temperature supercooling is further reduced because of the limited cell dimensions: The lateral extent of the fields around a growing crystal is related to the diffusion lengths d_T for the temperature field and d_C for the concentration field, where $d=2D/v$ and D is the relevant diffusion coefficient and v is the growth velocity. For steady-state growth conditions, the fields decay like $\exp(-x/d)$ away from the growth front. Orders of magnitude for d_T and d_C are 2 cm and 25–40 μm, respectively, for a typical velocity $v=0.1$ mm/s. Since the cell dimensions are $20<Z<160$ μm, usually $d_T\gg Z>d_C$. Now we can consider the copper base of the cell as an isotherm of solution temperature, and a simple calculation shows that the temperature of the crystal is essentially pinned by the isothermal boundary under these conditions. On the other hand, since $d_C<Z$ under most conditions of our experiments, the concentration changes are affected very little by the boundaries. Even when $d_C\sim Z$, since C satisfies Neumann boundary conditions at the cell walls, changes in C can be shown by the same calculation to be increased somewhat by the restricted geometry. These estimates indicate that only the concentration field needs to be considered in these experiments.

The considerations leading to the choice of a cell thickness are as follows. First, if the cell is thinner than d_C we should expect the concentration to be uniform across it and the growth to be essentially two dimensional. This means that the experiment will give full information about the diffusion field. But on the other hand, the limiting sensitivity is poor because of the small value of Z; for a 20-μm cell the minimum measurable δC is 0.77%, which is 10–15 % of the supersaturations used in the experiments. Now if we consider a thicker cell, the sensitivity will be greater, but the growth and diffusion is three dimensional and the values of δC obtained are averages of the concentration across the cell [Eq. (2)]. For a 160-μm cell, the minimum detectable δC is 0.1% of the average concentration across the cell. To emphasize this point, Fig. 3 shows the relative change in average concentration across the cell, at a fixed distance (50 μm) behind the tip of dendrites growing under similar conditions, as a function of the cell thickness. The local change δC next to the dendrite should be the same in all cases, but above 30-μm cell thickness ($Z\simeq d_C$), the contribution of the bulk fluid, which reduces the average value, becomes more and more dominant.

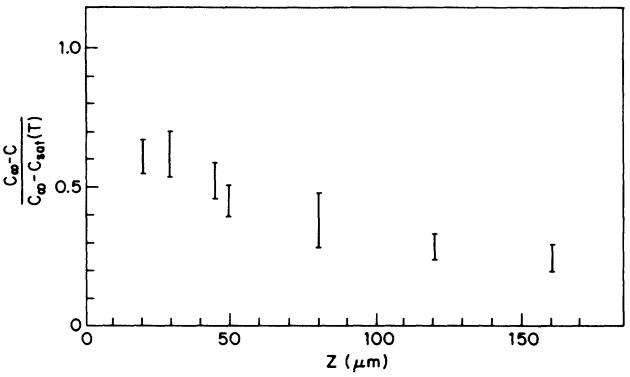

FIG. 3. Relative change in average concentration 50 μm behind the tip, as a function of cell thickness Z.

EXPERIMENTAL RESULTS AND ANALYSIS

Ammonium chloride can grow in three different modes, depending on the degree of supersaturation.[12] At the lowest supercooling, dendrites grow slowly in the ⟨100⟩ directions; at higher supercooling they grow first in the ⟨110⟩ directions and finally in ⟨111⟩ directions at the highest speed. The various modes can easily be recognized by the different angle between the side branches.

First we mention a quantitative verification of the reliability of the interferometric method. When the dendrite

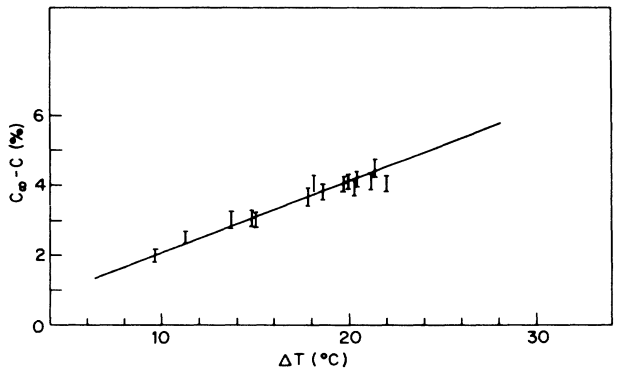

FIG. 4. Measurements of concentration on the surface far from the tip as a function of the supercooling. The line shows the saturation concentration.

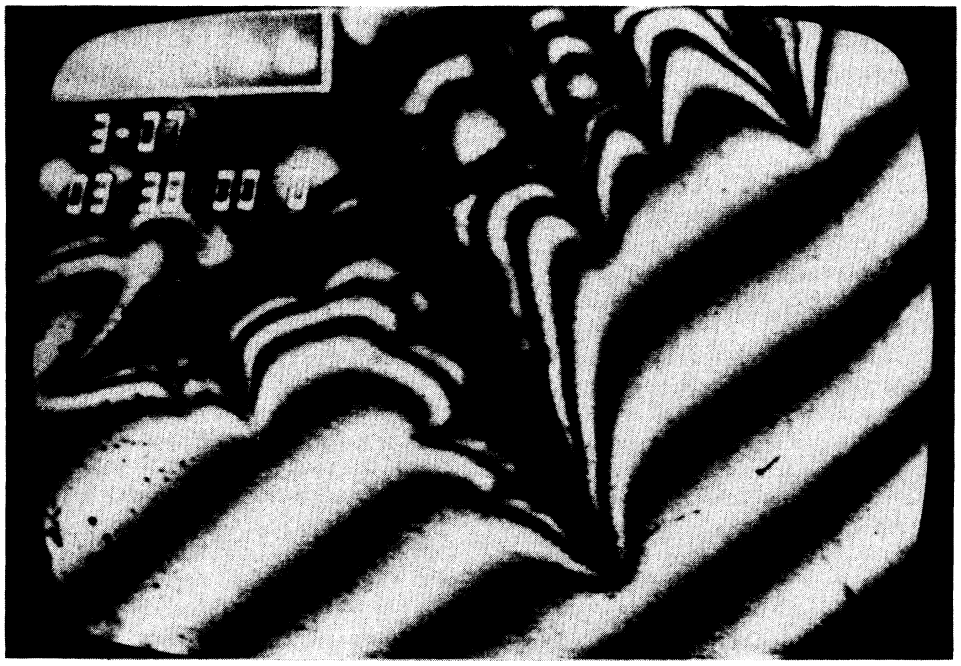

FIG. 5. Interferogram of a growing dendrite with side branches (photographed from the screen).

grows very slowly, we expect the solute concentration at its surface to be equal to the saturation value for the temperature of the sample. We measured the concentration difference between pairs of points, one close to the surface of the dendrite, well behind the fast-growing tip, and the other in the supersaturated fluid at a large distance ($\gg d_C$) from the dendrite. We confirmed that this difference corresponded to the known degree of supercooling. Note that under these conditions (slow enough growth) $d_C \gg Z$ and so there is no problem in integrating across the cell. The results of this investigation are shown in Fig. 4.

Figures 5 and 6 show typical interferograms around growing dendrites (the pictures shown are single frames

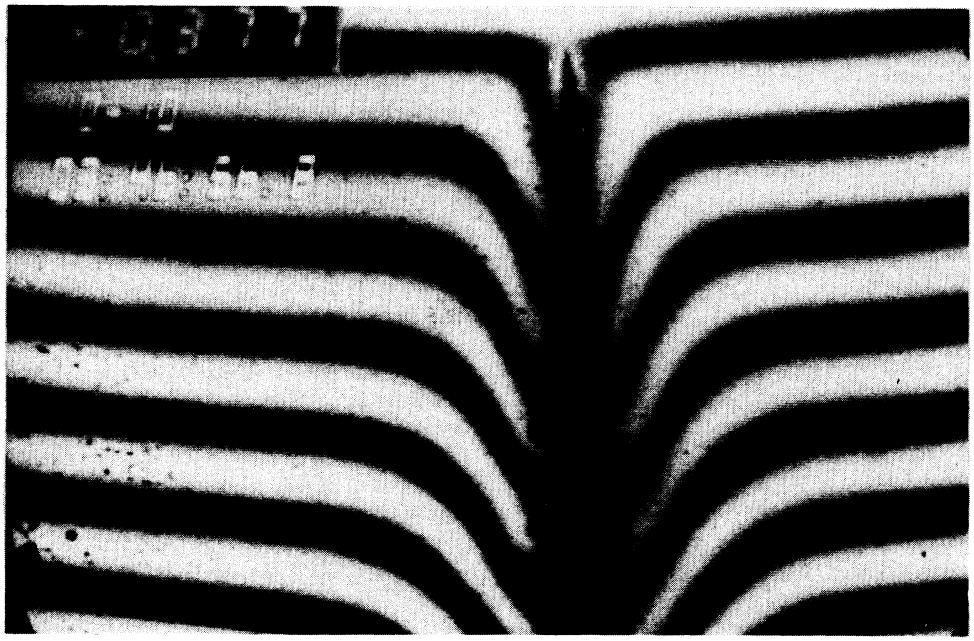

FIG. 6. Interferogram of an isolated growth stem (photographed from the screen).

from the video recording). Figure 5 shows a fairly complicated system with several side branches, whereas Fig. 6 illustrates a single growing stem before side branches form. This is a good example of a picture which is simple enough to be useful for a quantitative analysis. Figure 7(b) shows the mean concentration field as calculated from the fringe distortions. In this figure we can be misled into thinking that there is a considerable concentration gradient along the surface of the dendrite, but this is mainly an artifact of the averaging, since near the tip the system is not two dimensional, and there is also a gradient in the vertical direction.

In order to make a truer measurement of the real concentration in the proximity of the dendrite surface, it is necessary to correct for the solute distribution in the vertical direction. We chose to do this by comparing the experimental results with the model by McFadden and Coriell.[13] These authors have calculated the solute concentration field around an isotropically growing paraboloidal dendrite. Their model does not take into account capillarity (the capillary length in our experiments is 10^{-6} mm and therefore seems irrelevant—see Ref. 1), but does take into account the density difference between the two phases and therefore calculates a field which is not entirely diffusive. One should note that they assume the concentration at all points on the surface of the growing dendrite to be the saturation concentration.

McFadden and Coriell's solution is described by

$$C(\xi)=-1+\Gamma(-\epsilon p_e,p_e\xi^2)/\Gamma(-\epsilon p_e,p_e)\ , \tag{6}$$

where $\Gamma(a,b)=\int_b^\infty e^{-t}t^{a-1}dt$ is the complementary incomplete Γ function,[14] $p_e=vR/2D$ is the Peclet number, and $\epsilon=\rho_s/\rho_l-1$ is the fractional volume change on solidification, in which ρ_s and ρ_l are, respectively, the solid and liquid densities. The geometry is defined by parameter ξ which characterizes one of a family of paraboloids of revolution

$$y=\xi^2R/2-x^2/2R\xi^2\ , \tag{7}$$

where R is the tip radius and $\xi=1$ describes the paraboloidal surface of the dendrite.

The model clearly does not represent our situation exactly. First, the growth is not isotropic, since preferential growth in the ⟨100⟩ directions is clearly seen. Second, the shape of the dendrite is not exactly paraboloidal (it seem closer to a cone). However, there does not seem to be a better model for our purpose, and we do not believe that our conclusions are strongly dependent on it. Using this model, we can integrate in the z direction through the thickness of the cell and thus calculate the expected two-dimensional field, which we then compare with the experimental results. Figure 7(a) shows the calculated field, and Fig. 7(b) the measured one. The difference between the two fields is quite marked. It is clear that the averaging can account for only part of the apparent increase in concentration close to the tip of the growing dendrite which is evident in Fig. 7(b). We should remark that the existence of the upper and lower boundaries to the cell emphasize the discrepancy, since the boundary conditions tend to force the concentration in the direction of improved uniformity compared to the infinite medium.

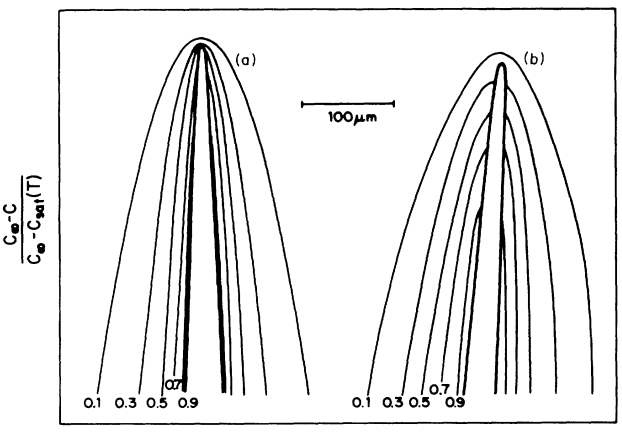

FIG. 7. Normalized concentration fields around an isolated stem (a) according to the theory (Ref. 13); (b) as measured. Absolute values can be obtained by multiplying by the total supercooling. The conditions of growth were bulk concentration $C_\infty=28.9\%$, growth velocity at the tip 170 μm s^{-1}, $T=9.1$ °C, $Z=47$ μm.

DISCUSSION

The results presented above suggest that the solute concentration on the dendrite surface is not a constant, but is greater than the solubility limit in the regions of fastest growth. Most recent theories of dendritic growth[2] assume that the supercooling at the interface is the bulk supercooling Δ modified by corrections for capillarity (curvature dependence) and a kinetic factor proportional to the normal growth velocity v_n:

$$u_s=\Delta-d_0\kappa-\beta v_n\ . \tag{8}$$

Since we have assumed that the capillary term is negligible, we concentrate our attention on the kinetic term, βv_n. The results of the experiments (Fig. 8) show that this term is not simply proportional to v_n. At growth velocities up to about 10 μm s^{-1} the assumption that the last term in (8) is proportional to v_n does seem to be valid; the value of β for the various examples is of order $0.2\%(\mu\text{m s}^{-1})^{-1}$ which, when u_s and Δ are normalized[12] as $(C-C_{sat})/C_{sat}$, is 8 s mm^{-1}. Above about 10 μm s^{-1} the linearity is clearly not valid. We consider that this result is consistent with a model in which the growth on a crystal surface is dominated by a nonlinear nucleation mechanism. This is the way in which a crystal surface grows at a temperature below its roughening temperature T_R. Although there is no measurement of T_R for any facet of NH_4Cl, photographs in the paper by Sawada[8] show faceting in the later stages of growth which suggest T_R to be above ambient. Indeed, the possibility of a nonlinear "kinetic factor" was mentioned by Ben-Jacob *et al.*[15] without specification of any particular model for this, and Dougherty *et al.*[5] have mentioned the need for specific consideration of nucleation mechanisms. It seems very likely that the existence of different supercool-

ing regimes for ⟨100⟩, ⟨110⟩, and ⟨111⟩ growth is another manifestation of the same model.

In a model for a growing crystal surface,[16] attachment of additional molecules to the surface only occurs at defects, which can be either the edges of thermally activated fluctuations in surface profile or structural defects. If the surface is atomically rough in its structure, i.e., at $T > T_R$, growth will occur for arbitrarily small values of supercooling (difference $\delta\mu$ in chemical potential between the solid and fluid phases) at a rate proportional to $\delta\mu$. At $T < T_R$, molecules can attach only around the edges of statistically generated islands on a surface. Provided that the island is larger than a certain limiting size, which depends critically on the degree of supercooling, the island grows; otherwise it shrinks. The result of this is a very nonlinear relationship between the rate of growth and the degree of supercooling at the surface:

$$v_n \sim \exp[-\pi\sigma^2/(kT\delta\mu)] , \tag{9}$$

where σ is the energy per unit length of the island perimeter, and is a function of T which becomes zero at the roughening temperature. The form of (9) can be represented crudely by a "nucleation barrier," by which we mean that if $\delta\mu$ is less than the barrier, there will be only very slow growth, whereas if $\delta\mu$ exceeds the barrier, growth is very rapid. In the slowly growing region the relationship (9) between $\delta\mu$ and v_n is not strictly linear. The magnitude of the barrier supersaturation can be estimated only if T_R and the solid-liquid surface tension are known, which they are not. Figure 8 shows the results of measurements of the growth velocity v_n as a function of the supersaturation next to the surface for ⟨111⟩ dendrites. It is clear that there is a strong nonlinearity reminiscent of a nucleation barrier. [We should remark that the actual reversal of $v(\delta\mu)$ in Fig. 8 is probably an artifact caused by the inapplicability in detail of McFadden and Coriell's solution[13] to this problem.] The barriers on differently oriented surfaces may be quite different, as may be the rates of growth once the barrier is exceeded.

Refinement of the roughening model by Van Saarloos and Gilmer[17] shows that under conditions far enough from equilibrium to allow several islands to grow simultaneously, the interface fluctuations resemble those of a rough surface even if $T < T_R$. This means that once fast growth on a surface has been initiated, it remains rough enough to facilitate further growth even if the value of $\delta\mu$ falls below the barrier. It will slow down only when $\delta\mu$ has become so small that the growth rate can no longer sustain the rough surface, which will occur at some lower level of supersaturation, and may be quite close to the saturation limit. Nozières and Gallet[18] have demonstrated similar behavior using renormalization theory. Moreover, Maurer *et al.*[3] have very recently suggested that growth-induced roughening occurs in NH_4Br from investigations of dendrite shape as a function of growth velocity.

The result of the growth mechanism described, together with diffusion of the solute in the fluid, is that growth of the crystal is not continuous but undergoes *relaxation oscillations.* Growth starts when the surface concentration exceeds the barrier, and it then continues until diffusion through the fluid is unable to maintain a level greater than the lower level. Growth then restarts only when the barrier level is exceeded again, at which point it can restart in any of several easy-growth directions, which means that side branches or a change in growth direction occur, depending on the exact concentration distribution over the surface.

The occurrence of side branches thus seems tied to the relaxation oscillations of the growth, and would thus seem to be periodic, at least in a system with distant boundaries. But the exact instant at which growth stops is a critical function of the local supersaturation which is the result of diffusion and is affected by the boundary conditions—among them the existing side branches, particularly the closest ones. An example would be a situation in which a large existing side branch inhibits diffusion, thus shortening the distance to the next side

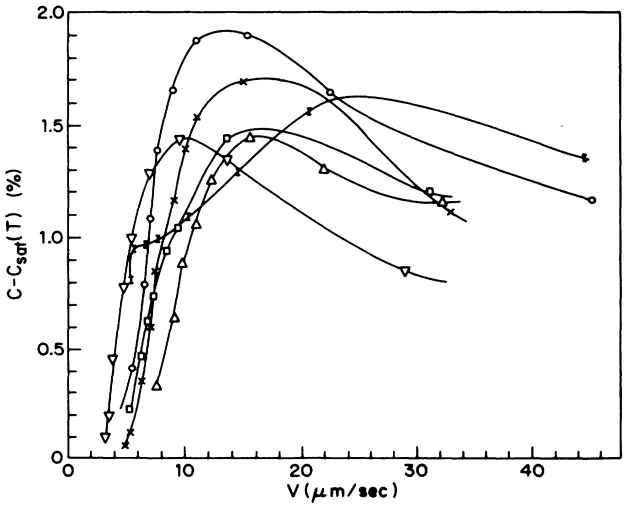

FIG. 8. Dependence of the discontinuity in C at the surface on the growth velocity v_n, for several crystals.

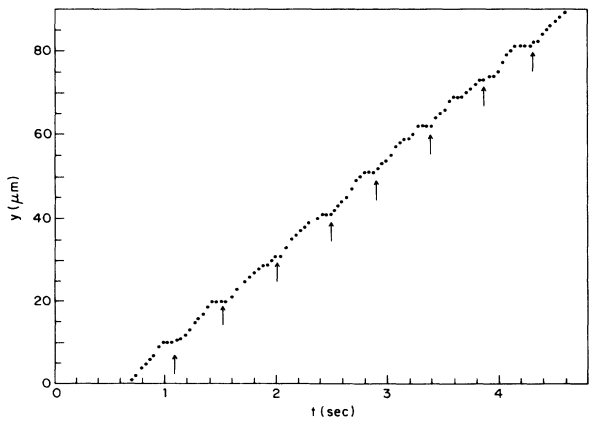

FIG. 9. Position of the dendrite tip as a function of time. The arrows represent the times at which side branches occurred. Notice the hesitation of the growth at these times.

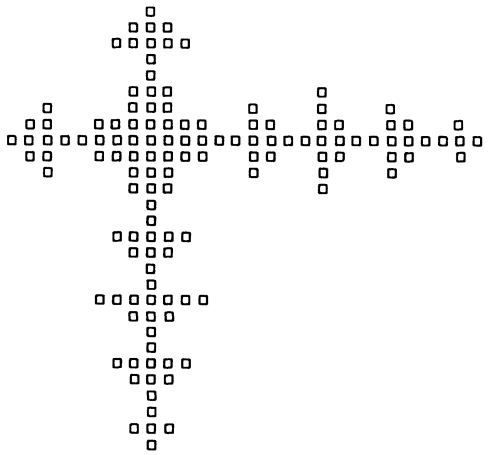

FIG. 10. Result of a simulation in two dimensions, based on the nucleation model.

branch, which then grows less because of the shadowing influence of the larger one. This is reminiscent of experiments on *LCR* circuits containing a diode with a current-dependent recovery time;[19,20] these undergo relaxation oscillations which are quasiperiodic and show a range of behaviors between periodicity and chaos. We suggest that dendritic growth, which also shows the range between periodicity and chaos[21,22] in side branching, is another example of a similar behavior. Statistical results on the spacing of side branches in NH_4Br dendrites have been published.[5]

Hints of the oscillations are observable in our experiments. We have measured the position of the tip of freely growing dendrites as a function of time, and can see the oscillatory behavior which correlates to the production of side branches. Figure 9 shows results for growth of a $\langle 100 \rangle$ dendrite in a cell 150 μm thick. The same behavior was remarked on by Honjo *et al.*[7] but since their experiments were done in a very thin cell (5 μm thick) we consider that the effect they observed may be due to interaction with the walls.[10] On the other hand, Dougherty *et al.*[5] claim that oscillations were not present in their very slowly growing dendrites.

We tried some naive two-dimensional (2D) simulations along these lines. A "crystal" grew on a square lattice, which initially had "supercooled fluid" at each point except for a single solid seed point. The crystal grew according to the following rules, applied to each cycle of the simulation. The liquid-solid interface is scanned. If an adjacent liquid point has concentration above a certain barrier, the solid grows into it, rejecting solvent into its neighborhood. If the solid had grown only in the previous cycle of the simulation, it can grow at a lower barrier. After each cycle, the solute redistributes in the fluid by diffusion for a certain time. Figure 10 shows the result after 19 cycles on a 30×30 grid, which shows quasiperiodic side branching. The tip hesitation phenomenon (Fig. 9) also occurs in the simulation. We confirmed that working on a finer grid (60×60) gave similar results after 19×4 cycles (in diffusion, which determines the time scale, $t\sim x^2$). This gives us a certain degree of confidence in the simulations, although they should in no way be considered as conclusive.

CONCLUSIONS

We have shown that the technique of interference microscopy can give a useful mapping of the concentration field around a growing dendrite. The results of our investigation of ammonium chloride indicate that there is a finite supersaturation of the fluid in contact with the growing surface of a crystal, and that the rate of growth is related to this supersaturation in a very nonlinear fashion. In addition, we find that the growth of the dendrite tip hesitates whenever a side branch emerges. Putting these facts together suggests that homogeneous nucleation theories for crystal growth on facets are applicable to the growth of these dendrites, and that the hesitation finds a natural explanation in terms in relaxation oscillations predicted by the growth dynamics. The relaxation oscillations also relate directly to pattern formation, and comparison with other systems with similar dynamics provides some insight into the variety of periodic and quasiperiodic forms that dendrites can assume.

ACKNOWLEDGMENTS

We are grateful to E. Ben-Jacob, S. Fishman, and M. Azbel for illuminating discussions and to D. Pengra for bringing Refs. 19 and 20 to our attention. We acknowledge the technical assistance of Y. Moses. This work was supported in part by the U.S.–Israel Binational Science Foundation and KLA Instruments, Inc.

[1]J. S. Langer, Physica A **140**, 44 (1986).

[2]For example, E. Ben-Jacob, N. D. Goldenfeld, B. G. Kotliar, and J. S. Langer, Phys. Rev. Lett. **53**, 2210 (1984).

[3]J. Maurer, P. Bouissou, B. Perrin, and P. Tabeling, Europhys. Lett. **8**, 67 (1989).

[4]M. E. Glicksman, R. J. Schaefer, and J. D. Ayers, Metall. Trans. A **7**, 1747 (1976); H. Chou and H. Z. Cummins, Phys. Rev. Lett. **61**, 173 (1988).

[5]A. Dougherty, P. D. Kaplan, and J. P. Gollub, Phys. Rev. Lett. **58**, 1652 (1987).

[6]S. K. Chan, H. H. Reimer, and M. Kahlweit, J. Cryst. Growth **43**, 229 (1978).

[7]H. Honjo, S. Ohta, and Y. Sawada, Phys. Rev. Lett. **55**, 841 (1985).

[8]Y. Sawada, Physica A **140** 134 (1986).

[9]J. Timmermans, *The Physico-Chemical Constants of Binary Systems* (Interscience, New York, 1960), Vol. 4, pp. 582–593; *Handbook of Physics and Chemistry,* 67th ed., edited by R. C. Weast (Chemical Rubber, Cleveland, 1986), p. D223; *Solubilities of Inorganic and Organic Compounds,* edited by H. Stephen and T. Stephen (Pergamon, London, 1963), Vol. 1, p. 213.

[10]E. Raz and S. G. Lipson (unpublished).

[11]W. Kurz and D. T. Fisher, *Fundamentals of Solidification* (Trans Tech, Aedermannsdorf, 1984).

[12]S. K. Chan, H. H. Reimer, and M. Kahlweit, J. Cryst. Growth

32, 303 (1976).
[13]G. B. McFadden and S. R. Coriell, J. Cryst. Growth **74**, 507 (1986).
[14]*Handbook of Mathematical Functions,* edited by M. Abramowitz and I. Stegun (National Bureau of Standards, Washington, D.C., 1964).
[15]E. Ben-Jacob, P. Garik, T. Mueller, and D. Grier, Phys. Rev. A **38**, 1370 (1988).
[16]J. D. Weeks and G. H. Gilmer, Adv. Chem. Phys. **40**, 157 (1979).
[17]W. van Saarloos and G. H. Gilmer, Phys. Rev. B **33**, 4927 (1986).
[18]P. Nozières and F. Gallet, J. Phys. (Paris) **48**, 353 (1987).
[19]R. W. Rollins and E. R. Hunt, Phys. Rev. Lett. **49**, 1295 (1982).
[20]R. V. Boskirk and C. Jeffries, Phys. Rev. A **31**, 3332 (1985).
[21]H. Honjo, S. Ohta, and M. Matsushita, J. Phys. Soc. Jpn. **55**, 2487 (1986).
[22]J. Bechhoefer and A. Libchaber, Phys. Rev. B **35**, 1393 (1987).

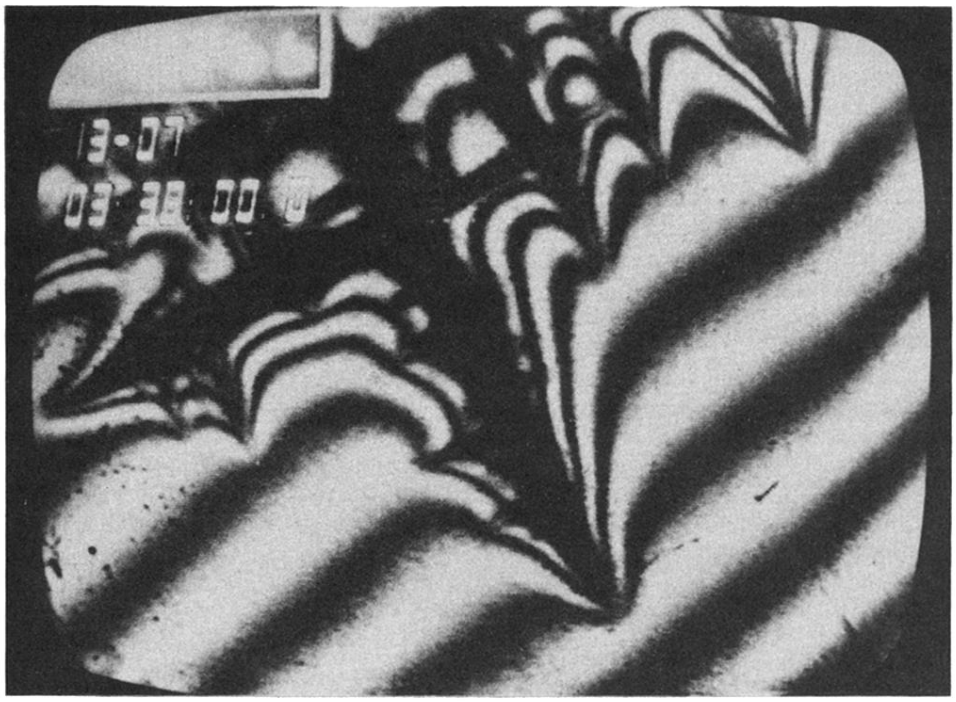

FIG. 5. Interferogram of a growing dendrite with side branches (photographed from the screen).

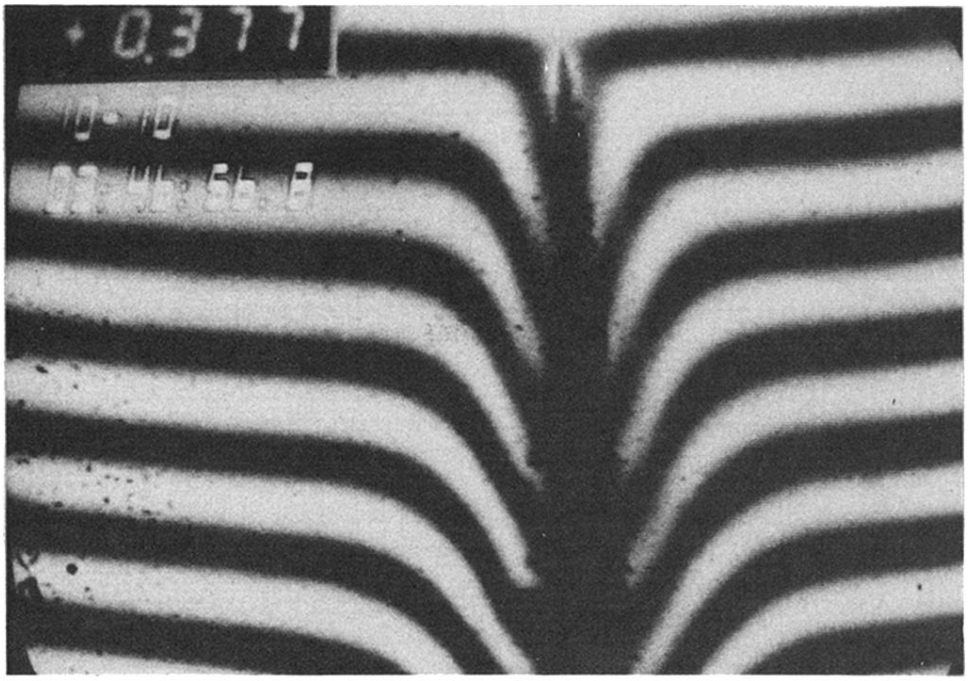

FIG. 6. Interferogram of an isolated growth stem (photographed from the screen).